

# Heparan Sulfate Proteoglycans Are Receptors for the Cell-surface Trafficking and Biological Activity of Transglutaminase-2<sup>§</sup>

Received for publication, March 19, 2009, and in revised form, April 24, 2009. Published, JBC Papers in Press, April 27, 2009, DOI 10.1074/jbc.M109.012948

Alessandra Scarpellini<sup>‡</sup>, Renée Germack<sup>‡</sup>, Hugues Lortat-Jacob<sup>§</sup>, Takashi Muramatsu<sup>¶</sup>, Ellen Billett<sup>‡</sup>, Timothy Johnson<sup>||</sup>, and Elisabetta A. M. Verderio<sup>‡1</sup>

From the <sup>‡</sup>School of Science and Technology, Nottingham Trent University, Clifton Lane, Nottingham NG11 8NS, United Kingdom, the <sup>§</sup>Institut de Biologie Structurale CNRS-CEA-UJF, 380272 Grenoble, France, the <sup>¶</sup>Department of Health Science, Faculty of Psychological and Physical Science, Aichi Gakuin University, Aichi 470-01953, Japan, and the <sup>||</sup>Academic Nephrology Unit, Medical School, University of Sheffield, Sheffield, S10 2RZ, United Kingdom

Transglutaminase type 2 (TG2) is both a protein cross-linking enzyme and a cell adhesion molecule with an elusive unconventional secretion pathway. In normal conditions, TG2-mediated modification of the extracellular matrix modulates cell motility, proliferation and tissue repair, but under continuous cell insult, higher expression and elevated extracellular trafficking of TG2 contribute to the pathogenesis of tissue scarring. In search of TG2 ligands that could contribute to its regulation, we characterized the affinity of TG2 for heparan sulfate (HS) and heparin, an analogue of the chains of HS proteoglycans (HSPGs). By using heparin/HS solid-binding assays and surface plasmon resonance we showed that purified TG2 has high affinity for heparin/HS, comparable to that for fibronectin, and that cell-surface TG2 interacts with heparin/HS. We demonstrated that cell-surface TG2 directly associates with the HS chains of syndecan-4 without the mediation of fibronectin, which has affinity for both syndecan-4 and TG2. Functional inhibition of the cell-surface HS chains of wild-type and syndecan-4-null fibroblasts revealed that the extracellular cross-linking activity of TG2 depends on the HS of HSPG and that syndecan-4 plays a major but not exclusive role. We found that heparin binding did not alter TG2 activity *per se*. Conversely, fibroblasts deprived of syndecan-4 were unable to effectively externalize TG2, resulting in its cytosolic accumulation. We propose that the membrane trafficking of TG2, and hence its extracellular activity, is linked to TG2 binding to cell-surface HSPG.

Transglutaminase type 2 (TG2,<sup>2</sup> EC 2.3.2.13) is the most widespread member of a large family of enzymes that catalyze the Ca<sup>2+</sup>-dependent post-translational modification of pro-

teins leading to intra- or intermolecular Nε(γ-glutamyl)lysine bonds (1, 2). Unlike other family members, TG2 is uniquely exported through a yet to be elucidated non-conventional pathway. Once secreted, TG2 finds in the extracellular compartment the ideal conditions of high Ca<sup>2+</sup> and low GTP concentration for the activation of its intrinsic transamidation activity (cross-linking) (2, 3). Intracellularly, GTP binding suppresses the Ca<sup>2+</sup>-dependent cross-linking activity and determines the additional GTPase activity of TG2 (4, 5), which is responsible for signal transduction (6). Once externalized, TG2 remains tightly bound to the cell surface and to the extracellular matrix (ECM) (7, 8), and it is rarely found free in the conditioned medium, unless overexpressed by cell transfection (9).

Extracellular TG2 activity is involved in the cross-linking of the ECM, conferring resistance to matrix metalloproteinase and promoting cell-matrix interactions via cross-linking of fibronectin (FN) and collagen (1, 7, 11, 12). TG2 has an additional non-enzymatic role in the matrix as an integrin-β<sub>1</sub> co-receptor (8) by supporting RGD-independent cell adhesion to FN (8, 13, 14).

Extracellular cross-linking and TG2-mediated adhesion facilitate the repair process in many tissue compartments (1, 2, 15, 16). On the other hand, uncontrolled cross-linking as a consequence of chronic cell insult and secretion of TG2 has been implicated in a number of pathological conditions, including kidney, liver, and pulmonary fibrosis (17–20).

Understanding how TG2 is exported and targeted to the cell surface is critical for limiting its cellular secretion and extracellular action. Although a key trigger for TG2 export is cell stress (2, 21, 22), TG2 is not unspecifically released, because extracellular trafficking occurs in the absence of leakage of intracellular components and cells remain viable (23). We know that TG2 requires the tertiary structure of its active site region to be secreted (9); moreover, TG2 is acetylated on the N terminus (24), a process reported to affect membrane targeting of non-conventional secreted proteins (25). Two main binding partners for TG2, FN and integrin-β<sub>1</sub>, have both been attributed a possible role in the transport of TG2 to the cell surface (8, 26). FN was shown to co-localize with TG2 once released (26), and integrin-β<sub>1</sub> to co-associate with TG2 in cells induced to differentiate (8).

TG2 has also long been known to have some affinity for heparin (27, 28), a highly sulfated analogue of heparan sulfate (HS)

<sup>§</sup> The on-line version of this article (available at <http://www.jbc.org>) contains supplemental Figs. S1–S8.

<sup>1</sup> To whom correspondence should be addressed: School of Science and Technology, Nottingham Trent University, Clifton Lane, Nottingham NG11 8NS, United Kingdom. Tel.: 44-(0)115-848-6628; Fax: 44-(0)115 848 6636; E-mail: [elisabetta.verderio-edwards@ntu.ac.uk](mailto:elisabetta.verderio-edwards@ntu.ac.uk).

<sup>2</sup> The abbreviations used are: TG2, transglutaminase type 2; GTPγS, guanosine 5'-3-O-(thio)triphosphate; ECM, extracellular matrix; FN, fibronectin; HS, heparan sulfate; HSPG, HS proteoglycan; FITC, fluorescein isothiocyanate; MDF, mouse dermal fibroblast; DMEM, Dulbecco's modified Eagle's medium; MEF, mouse embryonic fibroblast; HOB, human osteoblast; PBS, phosphate-buffered saline; BSA, bovine serum albumin; RU, resonance unit; TRITC, tetramethylrhodamine isothiocyanate.

## Heparan Sulfate Binding of Transglutaminase-2

glycosaminoglycan chains, which are abundant constituents of the cell surface/ECM. HS chains are linear polysaccharides consisting of alternating *N*-acetylated or *N*-sulfated glucosamine units (GlcNAc or GlcNS), and uronic acids (glucuronic acid GlcA or iduronic acid IdoA residues) (29), which only exist covalently bound to the core protein of cell-surface proteoglycans (syndecans and glypicans) and secreted proteoglycans (29). Heparin binding is a property common to many ECM proteins (29), but the level of affinity has never been established for TG2, which makes it difficult to estimate the real biological significance of this interaction. Heparan sulfate proteoglycans (HSPG) bind ECM ligands through the HS chains, influencing their biological activity, trafficking, and secretion. Among the HSPG subfamilies, the syndecans act as co-receptors for both ECM components and soluble ligands (30), and syndecan-4 has overlapping roles with extracellular TG2 in wound healing and fibrosis (31, 32). In this study, we show that TG2 has a surprisingly high affinity for heparin and HS, raising the hypothesis that HSPG are involved in its biological activity. We demonstrate that HSPGs are essential for the transamidating activity of TG2 at the cell surface and that syndecan-4 acts as a receptor for TG2, which is involved in the trafficking and cell-surface localization, and thus activity of TG2.

### EXPERIMENTAL PROCEDURES

**Equipment, Reagents, and Antibodies**—A 3000 Biacore system, CM4 sensor chips, amine coupling kit and HBS-P buffer were from Biacore AB. Biotin-LC-hydrazide was from Pierce. Highly purified guinea pig liver TG2 was obtained from N-Zyme (Darmstadt, Germany) and dissolved in 50 mM Tris-HCl, pH 7.4, containing 2 mM EDTA. Heparan sulfate from porcine intestinal mucosa was obtained from Celsus (Cincinnati, OH). Heparitinase (from *Flavobacterium heparinum*) was obtained from Seikagaku (Tokyo). Surfen (*bis*-2-methyl-4-aminoquinolyl-6-carbamide) was obtained from J. D. Esko (University of California, San Diego). Peptide P3 (purity > 95%) was synthesized by Activotec (Cambridge, UK). Monoclonal anti-TG2 antibodies TG100, Cub7402 and goat polyclonal anti-TG2 antibody Ab10445/50 were from Abcam; rabbit anti-syndecan-4 antibody was from Zymed Laboratories Inc./Invitrogen. Monoclonal anti-HS antibody 10E4 conjugated with fluorescein isothiocyanate (FITC) was from Seikagaku (Tokyo). Monoclonal Na<sup>+</sup>/K<sup>+</sup>-ATPase antibody was from Abcam (Ab7671). The other reagents, unless stated, were from Sigma-Aldrich.

**Cell Lines and Culture Conditions**—Wild type and syndecan-4<sup>-/-</sup> mouse dermal fibroblasts (MDFs) were isolated from skin biopsies of three months old C57BL/6 mice and syndecan-4<sup>-/-</sup> mice with C57BL/6 genetic background (33). Cells were maintained in Dulbecco's modified Eagle's medium nutrient mixture F-12 (DMEM-F12-HAM), supplemented with 10% fetal calf serum, 2 mM glutamine, non-essential amino acids, and penicillin/streptomycin (100 units/ml and 100 μg/ml, respectively). Wild-type and TG2<sup>-/-</sup> mouse embryonic fibroblasts (MEFs) (34) were donated by G. Melino (Leicester University, UK), and cultured as described above. Primary human osteoblasts (HOBs), obtained from femoral heads (35) (a gift from S. Downes and S. Anderson, University of Nottingham, School of

Biomedical Sciences), and HOB stably transfected with pSG5-TG and pSVneo (clone TG14) (36) (provided by M. Griffin, Aston University, UK) were maintained in DMEM supplemented as above. Swiss-3T3 cell lines capable of inducible expression of TG2 (clone TG3) (7) (provided by M. Griffin, Aston University, UK) were induced to express TG2 by 72-h culture in medium without tetracycline, as previously described (7, 26).

**Cell Transfections**—pcDNAhS4 was generated by subcloning full-length human syndecan-4 cDNA, excised from EcoRI/SalI sites of pBLShS4 (donated by M. Bass, Manchester University) into EcoRI/XhoI sites of pcDNA3.1(+). Transient transfection of pcDNAhS4 into syndecan-4-null MDF was performed by electroporation, using NucleofectorII (Amaxa), according to the manufacturer's instructions. Transfection efficiency was ≥60% when estimated by transfecting the reporter plasmid pEGFPN1 (Clontech).

**Reverse Transcription-PCR**—RNA was extracted from cells using RNeasy mini-Kit (Qiagen). Reverse transcription of DNase-treated RNA (1 μg) was performed using Superscript<sup>TM</sup>-II reverse transcriptase (Invitrogen) and oligo(dT) (Promega). For PCR, the following primers were used (5'→3'): tggaaagctgtggcgtgat and ccctgttctgttagccgtat (glyceraldehyde-3-phosphate dehydrogenase); gggggcattctaagtcag and taccgctatccccctacat (mouse syndecan-4); atgatgtccagattatgct and gcgtagaactcattggtgggg (human syndecan-4); agtatgagcattggcaacga and atacaggggatcggaaagtg (mouse TG2). The amplifications were conducted at 95 °C (60 s), 60 °C (45 s), and 72 °C (30 s), for 30 cycles. For syndecan-4, the annealing temperature was 54 °C.

**Analysis of TG2-heparin Interaction by Plate Binding Assay**—Low molecular mass heparin (4–6 kDa) or HS (12 kDa) was dissolved in PBS and immobilized on 96-well heparin-binding plates (BD Biosciences) according to the manufacturer's instructions. A concentration of 4.6 μM was shown to be optimal for assaying heparin-binding proteins using these plates (37). As positive and negative controls, FN (5 μg/ml) and BSA (5 μg/ml) were immobilized on tissue culture plates as described (13). The plate was washed three times with PBS and incubated with blocking solution (3% w/v BSA, in PBS, pH 7.4), for 1 h at 37 °C. After washing three times with PBS, plates were incubated with gpITG2 (0–212 nM), diluted in blocking buffer containing 2 mM EDTA, for 2 h at 37 °C. In some instance, EDTA was replaced by 2 mM CaCl<sub>2</sub> or supplemented by inactivating concentrations of GTPγ-S (100 μM). The plate was washed with PBS, and the bound TG2 was detected by an enzyme-linked immunosorbent assay-type assay using anti-TG2 antibody Cub7402 (13). Binding data were fit to "one site specific binding model" ( $R_2$  values of 0.95–0.98) using GraphPad Prism 5.0. The returned  $B_{max}$  values confirmed that the interactions between TG2 and heparin/HS were saturable.

**Analysis of TG2-heparin Interaction by Surface Plasmon Resonance**—Size-defined heparin (6 kDa), was biotinylated at its reducing end with Biotin-LC-hydrazide and immobilized on a Biacore sensorchip. For this purpose, two flow cells of a CM4 sensorchip were activated with 50 μl of 0.2 M *N*-ethyl-*N'*-(diethylaminopropyl)carbodiimide and 0.05 M *N*-hydroxysuccinimide, before injection of 50 μl of streptavidin (0.2 mg/ml in 10

mM acetate buffer, pH 4.5). The remaining activated groups were blocked with 50  $\mu$ l of ethanolamine (1 M, pH 8.5). Typically, this procedure permitted coupling of  $\sim$ 3500 resonance units (RU) of streptavidin. Biotinylated heparin (5  $\mu$ g/ml) in HBS containing 0.3 M NaCl was then injected across one flow cell to obtain an immobilization level of 50 RU. The other one was left untreated and served as a negative control. For binding assays, 80  $\mu$ l of purified TG2 (0–586 nM), diluted in EDTA-containing HBS-P buffer (10 mM Hepes, 150 mM NaCl, 2 mM EDTA, 0.005% (v/v) Surfactant P 20), at 25 °C, were simultaneously injected at a flow rate of 10  $\mu$ l/min (kinetic mode) across the control and heparin surfaces, after which the formed complexes were washed with running buffer for 5 min. The sensorchip surface was regenerated with a 1-min pulse of 0.025% SDS followed by a 5-min pulse of 2 M NaCl in HBS-P buffer. Control sensorgrams were subtracted on line from the heparin sensorgrams, and results were analyzed using the Bialva 3.1 software.

**Immunoprecipitations**—Confluent cell monolayers were detached using 2 mM EDTA in PBS, to preserve cell-surface proteins, and incubated for 1 h at 37 °C in the absence or presence of heparitinase (30 milliunits/ml) in serum-free medium. Cells were then homogenized in ice-cold hypotonic Tris-HCl buffer, pH 7.4, with protease inhibitors and after low speed centrifugation (to remove remaining whole cells and nuclei), crude plasma membranes were prepared as previously described (38). Protein estimation was performed using DC (Folin) assay (Bio-Rad). Equal amounts of membrane proteins (500  $\mu$ g) were then solubilized in lysis buffer containing 1% v/v IGEPAL CA 630, 1% v/v Triton X-100, 0.5% v/v deoxycholic acid, protease inhibitors and pre-cleared with protein-G-agarose incubation for 1 h at 4 °C. Membrane lysates were subjected to immunoprecipitation by incubation with rabbit anti-syndecan-4 antibody (against a syndecan-4-endopeptide) (2  $\mu$ g) or anti-TG2 antibody TG100 or, as a negative control, rabbit anti-gliadin antibody (2  $\mu$ g). In some instances the syndecan-4 immunoprecipitates were further incubated with 30 milliunits/ml heparitinase in lysis buffer at 37 °C for 1 h prior to further analysis. The immunocomplexes were separated by reducing SDS-PAGE (10% polyacrylamide) and immunoprobed with the antibodies against TG2, syndecan-4, or anti-human plasma FN antibody. Following incubation with the appropriate horseradish peroxidase-conjugated secondary antibody, bands were revealed by enhanced EZ-ECL chemiluminescence (Geneflow), using Fujifilm image analyzer-3000. Densitometry of the bands was conducted by Aida ID/evaluation 3.44.

**Detection of TG2 in Cell Fractions by Western Blotting**—Non-enzymatically detached cells were fractionated into membrane and cytosolic fractions as described above. Total and cell fraction lysates (30  $\mu$ g) were resolved by 4–20% gradient SDS-PAGE (Invitrogen) under reducing conditions, and TG2 was detected by Western blotting using anti-TG2 polyclonal antibody Ab10445/50 (1/1000) in blocking buffer (5% nonfat milk in TBST). TG2 was revealed by enhanced chemiluminescence, after incubation with rabbit anti-goat-horseradish peroxidase (Dako), as described above. Tubulin and Na<sup>+</sup>/K<sup>+</sup>-ATPase were

revealed as loading controls for cytosolic and membrane fractions, respectively.

**Flow Cytometry**—For flow cytometry, HOB cell monolayers were detached with 2 mM EDTA in PBS, pH 7.4. Live, non-permeabilized cells in suspension ( $2 \times 10^6$  cells/ml) were stained for cell-surface HSPG with anti-HS antibody 10E4 conjugated with FITC (8  $\mu$ g/ml), in serum-free DMEM medium for 2 h at +4 °C. After washing in serum-free medium, cells were fixed in 0.5% (v/v) formaldehyde, and analyzed in a Epics XL-MCL flow cytometer (Beckman-Coulter). In some instances, cells in suspension were pre-treated with heparitinase in serum-free medium, or kept in serum-free medium only, for 1 h at 37 °C, prior to staining of HS.

**Detection of Cell-surface TG2 Activity**—TG2 activity associated with the extracellular surface was assayed in live cells in culture by measuring the incorporation of biotin-cadaverine into FN, as described (7, 39). Briefly, cells were plated into 96-well plates ( $2 \times 10^4$  cells/well) precoated with plasma FN (5  $\mu$ g/ml) in serum-free DMEM (which contains an activating concentration of Ca<sup>2+</sup>), in the presence of the amine substrate biotinylated cadaverine (0.1 mM). Cells were allowed to adhere for 2 h at 37 °C, then washed with PBS, pH 7.4, containing 2 mM EDTA and incubated with 0.1% deoxycholate in PBS, pH 7.4, containing 2 mM EDTA. The biotinylated cadaverine incorporated into the deoxycholate-insoluble FN matrix was revealed by incubation with ExtrAvidin peroxidase followed by addition of 3,3',5,5'-tetramethylbenzidine at fixed time and stopped by 0.5 M H<sub>2</sub>SO<sub>4</sub>. Spectrophotometric absorbances were measured at 450 nm.

**Detection of TG2 Activity in Cell Fractions**—For detection of TG2 activity in cell homogenates and fractions we used the method described by Balklava *et al.* (9). TG2 activity in total and cell fraction homogenates was quantified by a modification of the cell-surface TG2 activity protocol, assaying 60  $\mu$ g of protein lysates. Cell lysates were incubated in FN-coated 96-well plates in the presence of 0.1 mM biotinylated-cadaverine, further supplemented with either 5 mM Ca<sup>2+</sup> or 2 mM EDTA. The level of incorporated biotin-cadaverine into FN was revealed as described above. Background TG2 activity values in the presence of EDTA were subtracted from activity values at 5 mM Ca<sup>2+</sup>. A standard curve of TG2 activity was obtained each time by assaying known quantities of purified TG2, diluted in serum-free DMEM in the same way.

**Fluorescent Staining**—For TG2 staining, cells were allowed to adhere on 8-well chamber slides ( $10^4$  MDF cells/well), in normal culture conditions (10% fetal calf serum-containing medium) for 2 h. Adhered cells were fixed in 3.7% (w/v) paraformaldehyde in PBS and permeabilized in 0.1% (v/v) Triton X-100. Fixed and permeabilized cells were blocked in 3% (w/v) BSA in PBS and then incubated with anti-TG2 antibody clone Cub7402 (2  $\mu$ g/ml) at +4 °C for 15 h, followed by rabbit anti-mouse IgG-FITC (Dako) diluted 1/100 at 37 °C for 2 h (7, 26). Specificity of Cub7402 was verified in TG2-null cells. Detection of actin stress fibers and TG2 was achieved by incubation of fixed and permeabilized cells with TRITC-labeled phalloidin (20  $\mu$ g/ml) in blocking buffer, which was added after incubation with Cub7402, together with the secondary antibody after extensive washings in PBS. Detection of syndecan-4

## Heparan Sulfate Binding of Transglutaminase-2

and TG2 was achieved by incubating the fixed and permeabilized cells with rabbit anti-syndecan-4 antibody (2  $\mu\text{g}/\text{ml}$ ) and Cub7402, at +4  $^{\circ}\text{C}$  for 15 h, followed by either anti-rabbit IgG-AlexaFluor488 and anti-mouse IgG-Rhodamine RedX (Invitrogen) (MDF cells) or donkey anti-rabbit IgG-AlexaFluor568 (Invitrogen) and sheep anti-mouse IgG-FITC (Dako) (diluted 1/100) (HOB cells). There is not overlap in emission spectrum of the fluorochromes used. To detect matrix-associated TG2, cells were incubated with the antibody in culture prior to fixation as described (7, 9). To visualize TG2 activity *in situ*, cells were seeded into 8-well glass chamber slides in the presence of 0.5 mM fluorescein-cadaverine (Molecular Probes, Eugene, OR), for a total of 15 h, as previously described (7, 9). Nuclei were stained using fluorochrome 4',6-diamidino-2-phenylindole or propidium iodide. Fluorescence images were obtained by a Leica TCSNT confocal laser microscope and corresponded to the central optical plane of the basal cell sections.

**Cell Attachment**—Serum-starved cells (maintained at 0.1% fetal calf serum for 15 h) were allowed to attach in serum-free medium to wells ( $10^4$  cells/well of 96-well plates) either coated with low molecular mass heparin (2.3–4.6  $\mu\text{M}$ ) or HS (1.2–4.6  $\mu\text{M}$ ) and, as positive and negative controls, coated with FN and BSA (5  $\mu\text{g}/\text{ml}$ ), respectively. The attached cells were fixed and stained with crystal violet; after extensive washes in PBS adherent cells were solubilized in 30% (v/v) acetic acid, and the absorbance was measured at 540 nm with a microplate reader (Bio-Rad) as described (9).

**Statistics**—All experiments were undertaken at least three times unless specified. Data are expressed as means  $\pm$  S.D. Differences between data sets were determined by the Student's *t* test (two-tailed distribution, two-sample equal variance).

## RESULTS

**Affinity of TG2 for Heparin/HS**—To study the interaction of TG2 with heparin, binding assays were developed by using heparin-coated plates where low molecular weight heparin is non-covalently immobilized to microtiter surfaces in a functionally active state (37). As previously described for TG2 bound to FN (13), TG2 was allowed to bind immobilized heparin in the presence of the  $\text{Ca}^{2+}$  chelator EDTA (2 mM) to prevent TG2 auto-transamidation. Purified TG2 displayed a concentration-dependent binding to heparin and the interaction with heparin was saturable (Fig. 1A). The affinity value of TG2 for heparin was in the low nanomolar range ( $K_d$  23.20  $\pm$  1.84 nM). TG2 binding to FN-coated wells and lack of binding to BSA were, respectively, a positive and a negative control for TG2 binding to heparin (Fig. 1B). The calculated affinity value for FN was 19.47  $\pm$  6.92 nM, a value aligned to that of past reports (40, 41). Incubation of TG2 with  $\text{Ca}^{2+}$  (2 mM) resulted in lower binding to immobilized heparin but the affinity remained high ( $K_d$  40.33  $\pm$  3.75 nM) (Fig. 1A). Incubation of TG2 with GTP $\gamma$ S, a non-hydrolyzable form of GTP that keeps TG2 in the close GTP-bound form (5), resulted in a comparable affinity binding ( $K_d$  44.54  $\pm$  10.04 nM) (Fig. 1A). Therefore, the slightly reduced affinity in the presence of  $\text{Ca}^{2+}$  is not the result of the  $\text{Ca}^{2+}$ -bound TG2 conformation. Instead, cations are likely to alter the conformation and dynamic properties of the heparin polysaccharide chains (42), thus justifying the slightly altered heparin

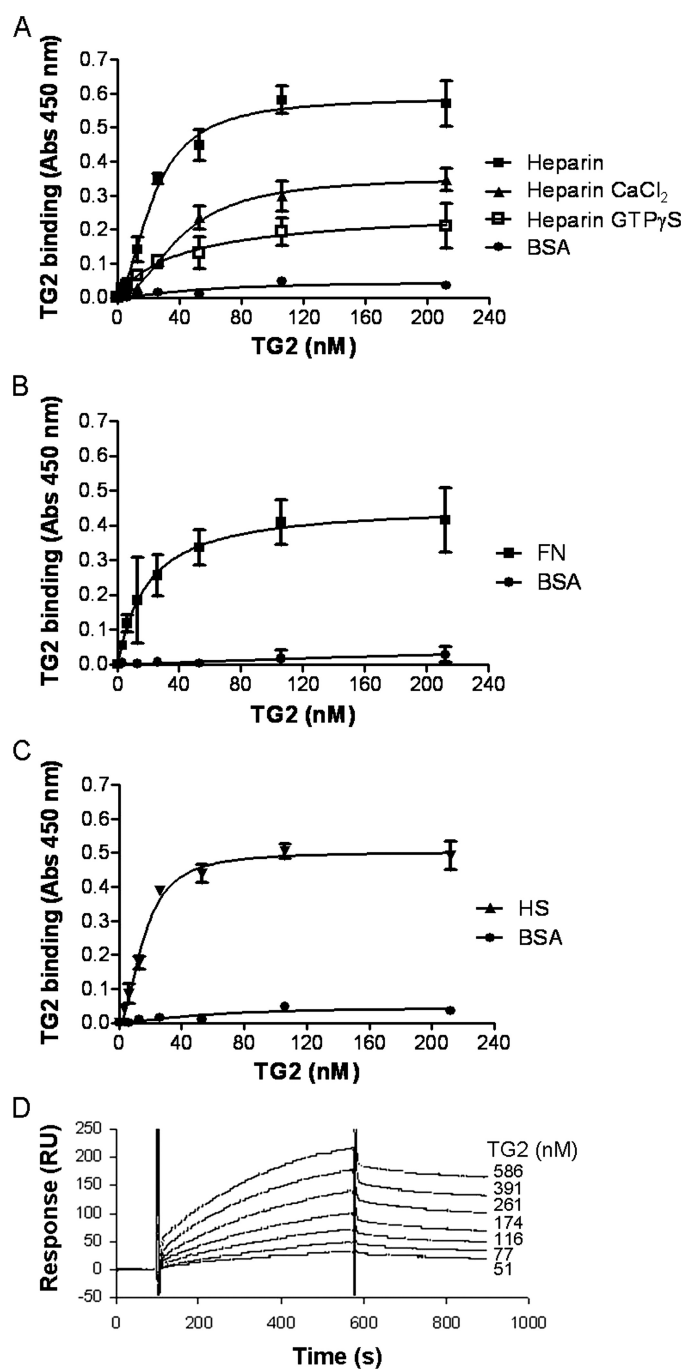


**FIGURE 1. TG2 binds immobilized heparin and HS.** A, the binding of purified TG2 to low molecular weight heparin was performed over 2 h at 37  $^{\circ}\text{C}$  in the presence of 2 mM EDTA, 2 mM  $\text{CaCl}_2$ , or 2 mM EDTA plus 100  $\mu\text{M}$  GTP $\gamma$ S, as described under "Experimental Procedures." The mean  $\pm$  S.D. of three independent experiments performed in triplicate is shown. B, binding assays to immobilized FN and BSA were used as positive and negative binding controls, respectively. C, binding of purified TG2 to immobilized HS was performed as described in A, in the presence of 2 mM EDTA. D, affinity of TG2 for heparin calculated by surface plasmon resonance. TG2 was injected over a heparin activated surface for 8 min at a flow rate of 10  $\mu\text{l}/\text{min}$ , after which running buffer was injected, and the response in RU was recorded as a function of time. Sensorgrams were obtained with increasing TG2 concentrations, and analyzed with the Biaeval 3.1 software.

recognition in the presence of  $\text{Ca}^{2+}$ . Similar heparin-binding curves to those obtained in the presence of  $\text{Ca}^{2+}$  were produced performing the assay in the presence of two other physiologically relevant cations ( $\text{K}^+$  and  $\text{Mg}^{2+}$ ) (supplemental Fig. S1).

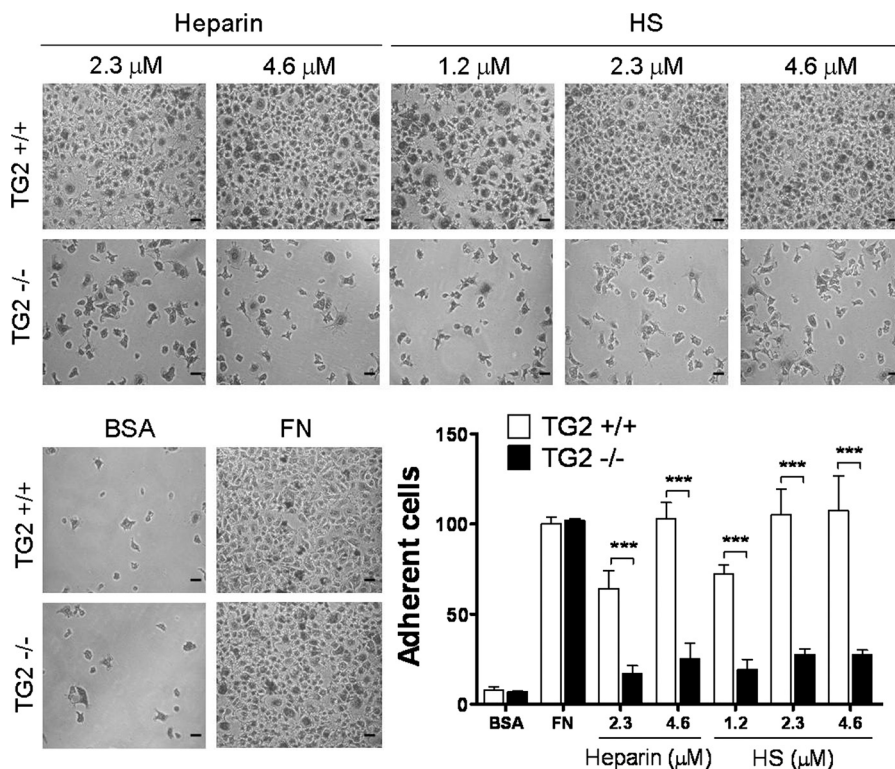


**FIGURE 2. Adhesion of wild-type (TG2<sup>+/+</sup>) and TG2-null (TG2<sup>-/-</sup>) MEF to immobilized heparin, HS, and control BSA.** Serum-starved cells were allowed to adhere for 1 h in serum-free medium, after that the attached cells were fixed, stained with crystal violet and quantified as described under "Experimental Procedures." Values are the mean  $\pm$  S.D. of a representative experiment performed in triplicate; data were normalized considering attachment of TG2<sup>+/+</sup> on FN as 100. \*\*\*, statistically significant differences in adhesion ( $p < 0.001$ ). The bars represent 20  $\mu$ m.

Heparin is commonly used as a substitute for HS in biochemical investigations (29). To examine whether the interactions between TG2 and HS were of similar strength as the interactions with heparin, solid binding studies were conducted using equimolar concentrations of purified HS. The TG2-HS interaction was saturable and was confirmed to be in the low nanomolar range ( $K_d$  15.92  $\pm$  0.96) (Fig. 1C). The interaction did not depend on the amount of HS as reducing HS to either one-half or to one-quarter returned a similar range of affinities (supplemental Fig. S2).

We further studied the TG2-heparin interaction using surface plasmon resonance, in the same conditions as the solid phase binding of TG2 to heparin/HS. Here the kinetic of binding was followed in real-time rather than at equilibrium as in the solid-binding assay. Heparin was coupled to a Biacore sensorchip, thus mimicking the cell-surface presentation of HSPG, and TG2 was perfused above this surface in the presence of 2 mM EDTA. Injection of increasing TG2 concentrations over a sensorchip activated with 50 RU of heparin gave rise to the binding curves shown in Fig. 1D. The  $A + B \leftrightarrow AB$  (Langmuir 1:1) model was first used to fit the data. This returned a "on" rate constant  $k_{on} = 5.5 \times 10^3 \text{ M}^{-1} \text{ s}^{-1}$  and a dissociation rate constant  $k_{off} = 4.95 \times 10^{-4} \text{ s}^{-1}$ , leading to an average dissociation constant of  $K_d = k_{off}/k_{on} = 92.7 \pm 4.7 \text{ nM}$ . Such a model returned a  $\chi^2$  value of 4.5, and this was not improved by fitting the data to other models. This data, taken together with the solid-binding assays, support the finding of high affinity of TG2 for heparin/HS.

**Recognition of Heparin/HS by Cell-surface TG2**—To investigate whether the TG2-HS affinity value is physiologically relevant we examined the recognition of heparin and HS by cell-surface TG2. We compared the level of attachment of wild-type MEFs and TG2-null MEFs to either heparin-coated or HS-coated plates, using FN and BSA coating as a positive and negative attachment control, respectively. Interference with pro-adhesive serum factors was ruled out by using serum-starved cells and omitting serum from the DMEM culture medium. DMEM contained 1.8 mM  $\text{Ca}^{2+}$ . In these conditions, wild-type and TG2-null MEFs displayed a similar level of attachment to FN and very low attachment to BSA (Fig. 2), although TG2-null MEF appeared less spread on FN. Conversely, wild-type MEFs had a significantly higher level of attachment to either heparin or HS, compared with TG2-null MEFs (Fig. 2). This finding suggests that cell-surface TG2 interacts with heparin/HS in

the presence of activating concentrations of  $\text{Ca}^{2+}$ .

**Direct Co-association of Cell Membrane TG2 with the HS Chains of Syndecan-4**—The biological significance of the binding to heparin was then studied by co-immunoprecipitation analysis of TG2 and the HS cell-surface receptor syndecan-4 in different cell types. To examine whether TG2 can act as a ligand for syndecan-4, membrane preparations of human osteoblasts (HOB), which are rich in HSPG (43) and express cell-surface TG2 (36, 44), were subjected to immunoprecipitation analysis. The expression of syndecan-4 was firstly analyzed by Western blotting of HOB membrane lysates using antibody against syndecan-4 core protein, which revealed a diffuse polypeptide of approximate 200 kDa (supplemental Fig. S3, asterisk) and other diffuse bands of approximate 90, 65, and 40 kDa. The 200-kDa band was eliminated by enzymatic digestion with heparitinase (45) and resulted in the clearing of the smear and intensification of the 40-kDa band (supplemental Fig. S3, arrow), which should correspond to the syndecan-4 core protein homodimer (46, 47). For immunoprecipitation, firstly, HOB membrane lysates were incubated with either rabbit anti-syndecan-4 antibody or control rabbit anti-gliadin antibody, and then the immunoprecipitated proteins were analyzed by Western blotting with mouse anti-TG2 antibody (Fig. 3A). The membrane-located endogenous TG2 was specifically co-immunoprecipitated with endogenous syndecan-4 in HOB (Fig. 3A, arrowhead). Transfected human TG2 was also found to be associated with endogenous syndecan-4 in the stably transfected HOB cell line TG14 (36) (Fig. 3A, arrowhead). As a control of syndecan-4 immunopre-

## Heparan Sulfate Binding of Transglutaminase-2

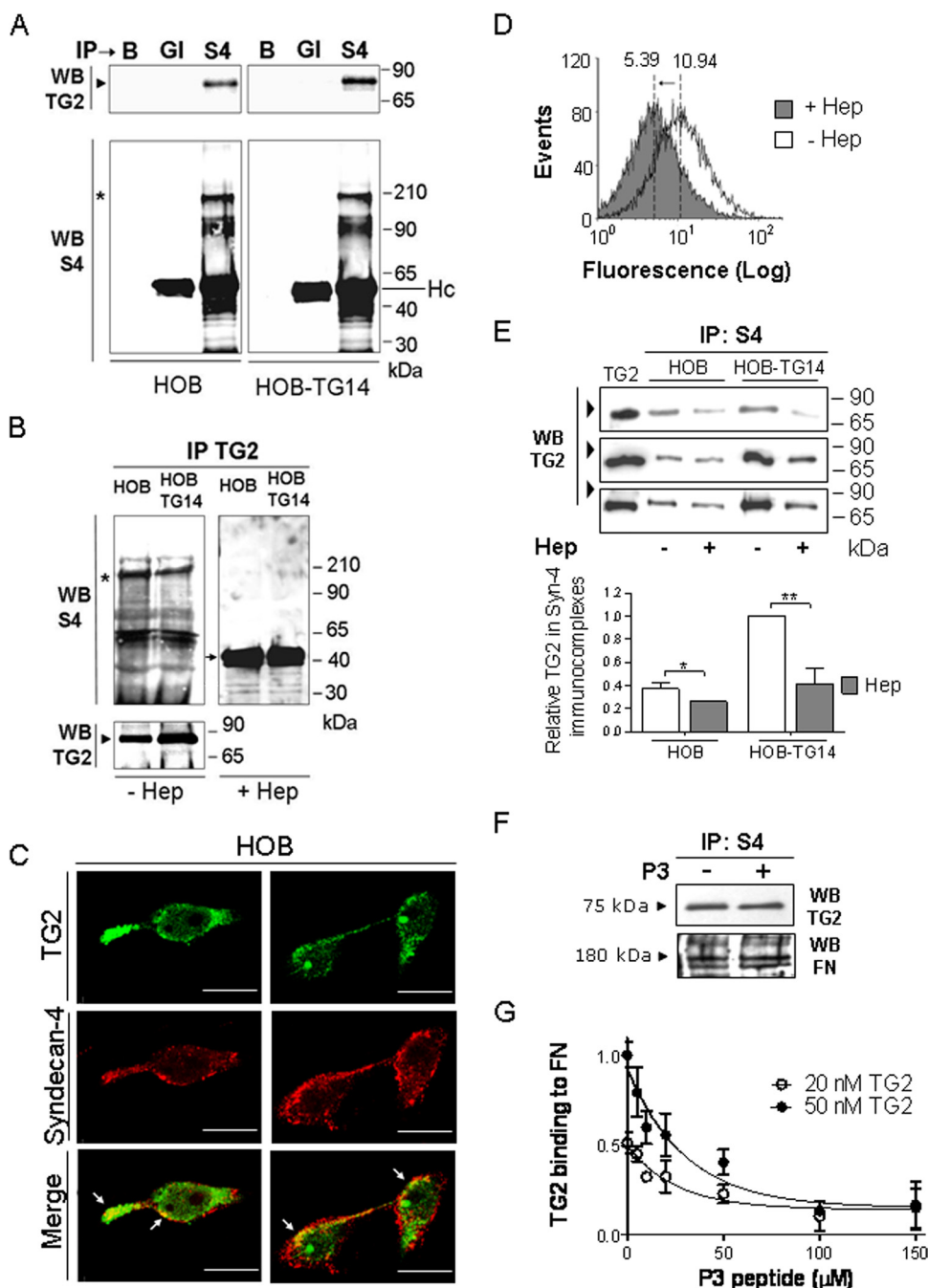


**FIGURE 3. Association of TG2 to syndecan-4.** *A*, membrane lysates from wild-type and TG2-transfected HOB (HOB-TG14) were immunoprecipitated with anti-syndecan-4 antibody (S4) and, as negative controls, anti-gliadin antibody (GI) or protein G-Agarose only (B). Immunoprecipitates were subjected to Western blot analysis for TG2 and syndecan-4. Arrowhead indicates TG2; asterisk, glycanated S4 (~200 kDa); Hc antibody heavy chain (~50 kDa). *B*, the same membrane lysates were immunoprecipitated with anti-TG2 antibody, digested or not with heparitinase (Hep) and subjected to Western blot analysis for syndecan-4 and TG2. Arrow, S4 core protein dimer. *C*, TG2 and syndecan-4 co-localization in HOB. TG2 was detected by mouse anti TG2 antibody and syndecan-4 with rabbit anti syndecan-4 antibody followed by sheep anti-mouse IgG FITC and donkey anti-rabbit IgG AlexaFluor568. Two separate fields are shown. Co-localization is pointed by the arrows. The bar indicates 20  $\mu$ m. *D*, flow cytometry of live HOB stained with a FITC-conjugated monoclonal anti-HS chains antibody, before and after heparitinase (Hep) digestion of HS. The arrow indicates the shift of mean fluorescence. *E*, the syndecan-4 immunoprecipitates described in *A* were repeated using membrane preparations from cells preincubated or not with heparitinase (Hep) prior to immunoprecipitation. TG2 indicates 200 ng of standard purified TG2. Three replicate blots are shown, and quantification of syndecan-4 co-immunoprecipitated TG2 is presented in the histogram. Arrowheads point to TG2 standard  $\pm$  S.D. \*,  $p < 0.05$ ; \*\*,  $p < 0.01$ . *F*, the syndecan-4 immunoprecipitations described in *A* were conducted in the presence of peptide P3 that mimics the FN binding site within TG2. Arrowheads indicate TG2 or FN co-immunoprecipitated with syndecan-4. *G*, inhibition of TG2-FN binding, assayed using 20 nM and 50 nM purified TG2 on FN in the presence of increasing concentrations of peptide P3. The experiments were repeated at least three times.

precipitation, the membranes were stripped and re-probed with anti-syndecan-4 antibody. Syndecan-4 was mainly detected in the high molecular weight range (~200 kDa, Fig. 3A, asterisk) corresponding to the glycanated form of syndecan-4. This result was similar to that of a previous report (48), and bands could be distinguished only after a very short blot development (Fig. 3A). The antibody chains were also detected, as expected, in the immunoprecipitates with rabbit antibodies. Secondly, membrane lysates were incubated with mouse anti-TG2 antibody, and the immunoprecipitated proteins were analyzed by Western blotting with rabbit anti-syndecan-4 antibody (Fig. 3B). Syndecan-4 co-precipitated with membrane TG2 in both transfected and untransfected HOB (Fig. 3B, asterisk). Identification of the 200-kDa polypeptide and lower molecular-size bands as syndecan-4 was shown by treatment of the immunoprecipitates with heparitinase, which eliminated these bands and revealed the core protein dimer of approximate 40 kDa (Fig. 3B, arrow). As a control of TG2 precipitation, the stripped membranes were re-probed with anti-TG2 antibody showing a protein of the expected size (~75 kDa) (Fig. 3B, arrowhead). TG2 association with syndecan-4 was verified by dual immunofluorescent staining of TG2 and syndecan-4 in HOBs, which were found to co-localize at the cell border and in cells' tail (Fig. 3C, arrows).

To investigate whether TG2 bound to the HS chains of syndecan-4, cells suspensions were incubated with heparitinase, which leads to specific degradation of cell-surface HS, prior to immunoprecipitation of syndecan-4. Flow cytometry analysis of HS after heparitinase treatment demonstrated cleavage of HS chains in about half the HS from HOB cells in suspension (Fig. 3D). Removal of cell-surface HS chains proportionally decreased the level of TG2 associated with syndecan-4 immunoprecipitates (Fig. 3E, arrowheads), suggesting

that the majority of TG2 binding is mediated by the HS chains of syndecan-4.

To investigate whether syndecan-4 was co-associated with cell-surface TG2 also in fibroblasts, we utilized a Swiss 3T3 cell line with tetracycline-regulated inducible expression of TG2 (7). We found that membrane-located endogenous TG2 co-immunoprecipitated with syndecan-4 (supplemental Fig. S4A), and this co-association was confirmed in membrane preparations of cells induced to overexpress TG2 by tetracycline withdrawal (supplemental Fig. S4A). Similarly to HOB cells, removal of HS from Swiss 3T3 fibroblasts decreased the level of TG2 associated with syndecan-4 immunoprecipitates (supplemental Fig. S4B).

Because the Hep II domain of FN associates with the HS chains of syndecan-4, and FN is also a high affinity binding partner of TG2, it could reasonably mediate the TG2-syndecan-4 interaction. To examine this possibility we interfered with TG2-FN binding using competitive concentrations of a synthetic peptide that mimics the FN binding site within TG2 (P3) (40). HOB cells were plated on a FN matrix preincubated with peptide P3 (100  $\mu\text{M}$ ) prior to cell seeding. After 1 h, both adherent and non-adherent cells were collected, and membrane preparations subjected to immunoprecipitation with anti-syndecan-4 antibody (Fig. 3F) followed by Western blotting with anti-TG2 or anti-FN antibody. Displacement of TG2 from FN did not lead to a decrease in the level of TG2 associated with syndecan-4 (densitometric values with and without 100  $\mu\text{M}$  P3 were  $1.2 \pm 0.18$  and  $1.0 \pm 0.07$ , respectively,  $p = 0.32$ ) (Fig. 3F). Western blot analysis of FN in syndecan-4 immunoprecipitates also revealed no changes in FN (densitometric values with and without P3 were  $1.0 \pm 0.14$  and  $1.0 \pm 0.11$ , respectively,  $p = 0.86$ ) (Fig. 3F). Control plate assays of TG2-FN binding, confirmed that incubation of two different concentrations of purified TG2 with increasing concentrations of P3 (0–150  $\mu\text{M}$ ) led to a significant inhibition of TG2 binding to FN (Fig. 3G). In conclusion, our findings suggest the direct association of TG2 with the HS chains of syndecan-4.

**HS Chains Influence TG2 Activity at the Cell Surface**—To examine whether the association of TG2 with HS chains, particularly those of syndecan-4, influences TG2 cell-surface cross-linking activity, primary MDFs were chosen as a model, because MDFs with targeted deletion of syndecan-4 were available to us. Moreover, the components of the dermal matrix, such as type I/III collagen, fibrillin-1, and FN are all major substrates of TG2 transamidation (11, 12, 49, 50). TG2 extracellular activity was measured in live cells in culture by using a previously described plate assay (7, 39). In a first set of experiments, wild-type MDF (MDF S4<sup>+/+</sup>) were treated to reduce their level of cell-surface HS by either incubation with heparitinase or surfen (12  $\mu\text{M}$ ), a general antagonist of HS (51). A significantly lower level of TG2 transamidation was found at the surface of wild-type MDF pre-treated with both heparitinase and surfen compared with untreated cells (Fig. 4A). Titration of the cell-surface TG2 inhibition effect by surfen revealed an  $\text{IC}_{50}$  of 6.8  $\mu\text{M}$  (supplemental Fig. S5). Any possible interference of surfen with the cell-surface TG2 activity assay itself (incorporation of biotin cadaverine into FN) was ruled out by producing statistically similar dose-response curves of TG2 activity when using

purified TG2 in the absence and in the presence of 6 and 12  $\mu\text{M}$  surfen (supplemental Fig. S6). When the role played by syndecan-4 was investigated, a significantly lower level of TG2 activity was measured at the surface of syndecan-4-null MDF (MDF S4<sup>-/-</sup>) compared with wild-type MDF (Fig. 4A). The total level of TG2 expression was found to be statistically similar in wild-type and syndecan-4-null MDF when assayed by reverse transcription-PCR of total RNA, or total TG2 activity assay, or Western blotting of the whole cell lysates (Fig. 4B). This finding indicates that the loss in cell-surface TG2 activity in syndecan-4-null MDF is not due to a change in total TG2. The residual level of extracellular TG2 was significantly higher in syndecan-4-null MDF than in surfen or heparitinase-treated wild-type MDF (Fig. 4A), and both surfen and heparitinase treatments significantly lowered cell-surface TG2 in syndecan-4-null cells (Fig. 4A), suggesting that syndecan-4 is not the only HSPG implicated with extracellular TG2 activity. To test TG2 activity in syndecan-4-null MDF with added-back syndecan-4, we cloned syndecan-4 cDNA in the mammalian expression vector pcDNA3.1 and confirmed its expression in syndecan-4-null MDF transfected with this construct (Fig. 4C). Reconstitution of syndecan-4 in syndecan-4-null MDF restored cell-surface TG2 activity to wild-type levels (Fig. 4A). Conversely, heparitinase or surfen treatment of the syndecan-4-null MDF with reconstituted syndecan-4 further inhibited extracellular TG2 activity (Fig. 4A), thus confirming the role of the syndecan-4 HS chains. Therefore, the present findings demonstrate that syndecan-4 significantly affects the extracellular activity of TG2, but other HSPG are also involved.

The plate assay of TG2 activity in live cells in culture was developed to detect the whole extracellular TG2 activity, either located at the cell surface or bound to FN in 2 h cell adhesion to FN (7, 39). To rule out the possibility that the deficiency in extracellular TG2 found in cells either lacking functional HS or syndecan-4 could be due to improper engagement of cells with FN, we quantified the attachment of surfen-treated wild-type and syndecan-4-null MDF in serum-free conditions. As shown in Fig. 4D, neither syndecan-4 deletion nor surfen treatment significantly altered MDF attachment to FN in 2 h. Treatment with heparitinase was also shown not to diminish cell attachment to FN (13), thus confirming that the deficiency in TG2 is not due to an alteration of cell-substratum interaction.

To visualize extracellular TG2 activity, cells were seeded and grown for 15 h in medium containing a cell-permeable fluorescent amine TG substrate (fluorescein-cadaverine) as previously described (7, 9). Fluorescein-cadaverine was found to be predominantly cross-linked in cell-matrix glutaminy substrates and in the pericellular matrix of wild-type MDF (Fig. 5). Syndecan-4-null cells displayed a significantly lower level of *in situ* TG2 activity compared with wild-type cells (Fig. 5), in agreement with measurements of cell-surface TG2 by plate assay (Fig. 4A). To verify that TG2 activity was responsible for the fluorescent signal, a specific site-directed inhibitor of TG, R-283, which targets the Ca<sup>2+</sup>-activated form (9), was utilized in negative control experiments, showing a drastic inhibition of the *in situ* TG reaction in both wild-type and syndecan-4 null MDF (Fig. 5). The specificity of the *in situ* reaction for TG2 was

## Heparan Sulfate Binding of Transglutaminase-2

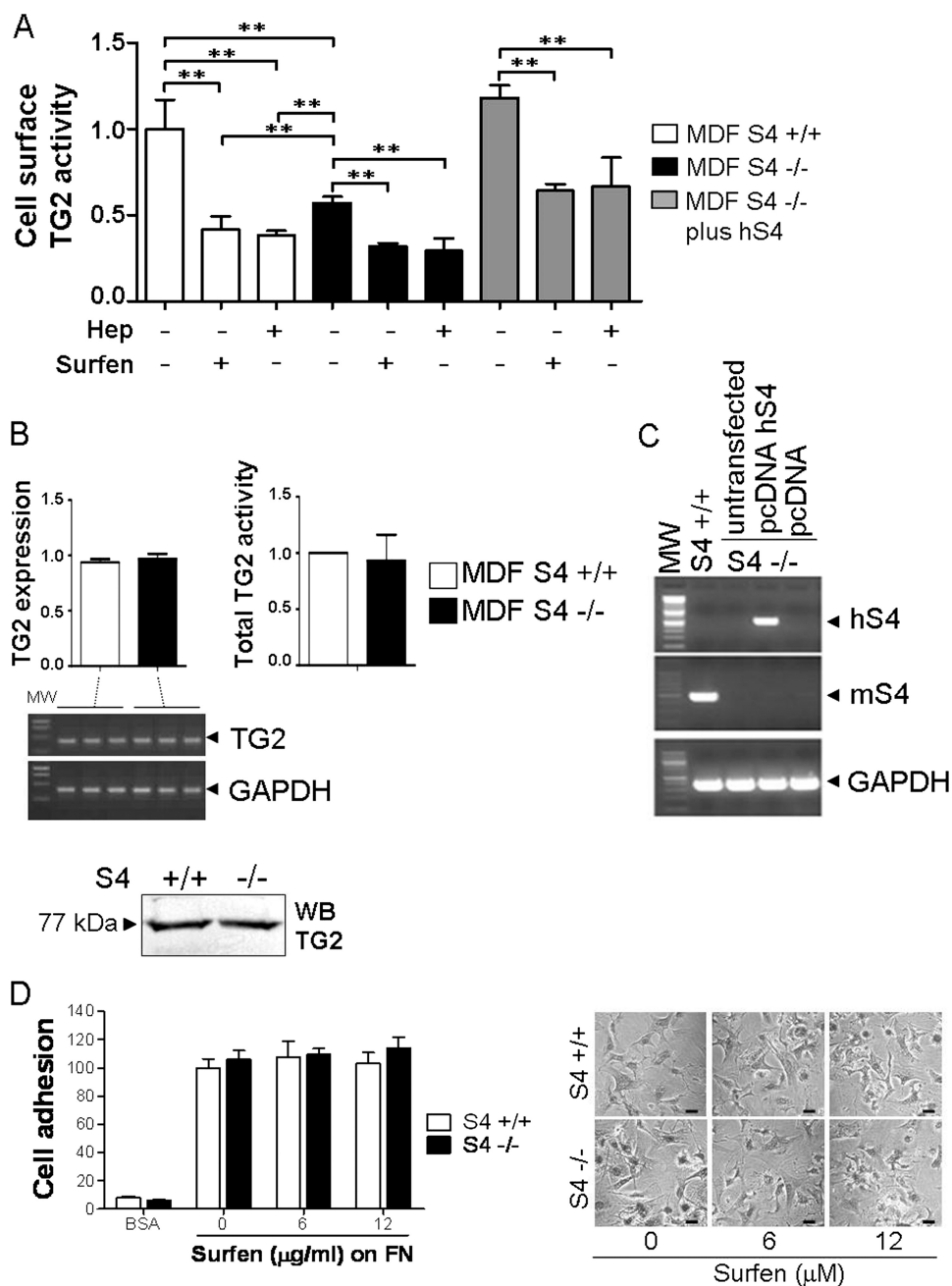


**FIGURE 4. Cell-surface HS affect extracellular TG2 activity of primary dermal fibroblasts adherent to FN.** *A*, cell-surface TG2 activity was measured in wild-type ( $S4^{+/+}$ ), syndecan-4-null ( $S4^{-/-}$ ), and syndecan-4-null MDF with added-back S4 by cell transfection of pcDNAhS4. In some instances, cells were either pretreated with heparinase (*Hep*) or with the HS antagonist surfen ( $12 \mu\text{M}$ ) or incubated with medium only, for 1 h at  $37^\circ\text{C}$ . Afterward cells were seeded on FN and assayed for TG2 activity in the presence of *Hep* or surfen. The cell-surface TG2 activity was expressed as normalized mean absorbance at  $450 \text{ nm} \pm \text{S.D.}$ , using wild-type untreated samples as normalizers (typical optical density = 0.6). \*\*, statistically significant decrease in cell-surface TG2 activity ( $p < 0.01$ ). *B*, the expression of TG2 in wild-type and syndecan-4-null MDF was analyzed by reverse transcription-PCR, using triplicate samples of total RNA/cell type, followed by quantification of bands intensities by densitometry. Values (TG2 expression) are mean ratios of TG2 intensity versus control glyceraldehyde-3-phosphate dehydrogenase (*GAPDH*). The expression of total TG2 in cell homogenates was evaluated by means of a TG2 activity plate assay (Total TG2 activity), as described under "Experimental Procedures." TG2 activity data represent mean values  $\pm \text{S.D.}$  of three separate experiments, using values of wild-type cells (typical optical density = 0.5) as normalizers. TG2 expression was also analyzed by Western blotting of total cell homogenates using polyclonal anti-TG2 antibody Ab10445/50. *C*, re-expression of syndecan-4 (*hS4*) in syndecan-4-null MDF was tested by reverse transcription-PCR on RNA isolated 48 h after transfection of pcDNAhS4 or the empty vector pcDNA. Endogenous mouse syndecan-4 (*mS4*) was detected in wild-type MDF ( $S4^{+/+}$ ). Expression of glyceraldehyde-3-phosphate dehydrogenase was monitored to confirm equal loading of RNA. *MW*, molecular DNA markers (1-kb Promega). *D*,  $S4^{+/+}$  and  $S4^{-/-}$  MDF were allowed to attach to FN-coated wells, in the same conditions as in the cell-surface TG2 assay described in *A* (in serum-free conditions), but in the absence of amine substrate. Where indicated, cells had been incubated with 6 and  $12 \mu\text{M}$  Surfen. At the end of the 2-h incubation, cell attachment was quantified as described under "Experimental Procedures." The bars indicate  $20 \mu\text{m}$ .

confirmed by the absence of fluorescence in  $TG2^{-/-}$  MEFs compared with wild-type MEFs (supplemental Fig. S7A).

**Defects of TG2 Export in Syndecan-4-null MDF**—After showing that the HS chains are critical for the biological activity of TG2 at the cell surface, and that TG2 directly binds to the HS chains of syndecan-4, we investigated whether HS binding had a direct influence on the enzymatic activity of TG2 or, alternatively, on the cell trafficking/localization of TG2. To address the first hypothesis we assayed the  $\text{Ca}^{2+}$ -dependent transamidation of purified TG2 in the presence and absence of heparin. As shown in Fig. 6, heparin did not significantly alter the cross-linking activity of a range of TG2 concentrations (2–8 nM), chosen to be similar to the level of TG2 we estimated to be present at the surface of MDF (data not shown).

We then tested whether the removal of HSPG, and in particular syndecan-4, may interfere with TG2 exposure at the cell surface. In a first set of experiments we undertook immunofluorescent staining of TG2 in fixed and permeabilized MDF with or without syndecan-4. TG2 was found to be predominantly located at the cell periphery of wild-type MDF, concentrated at the basal surface (Fig. 7A, arrows). Instead, staining of syndecan-4-null MDF revealed a marked reduction in TG2 at cell/matrix contacts, which was accompanied by an increase in the cytosolic staining (Fig. 7A). Using double fluorescence labeling, we verified that anti-TG2 antibody labeled large peripheral cell-matrix adhesions, which appeared to be connected to the end of actin filaments, as shown by the merged images (Fig. 7B, arrowheads). In addition, the anti-TG2 antibody decorated extracellular structures (Fig. 7B, small arrows), consistent with TG2 secretion. The localization of TG2 at focal adhesions and in the pericellular matrix was previously described (8, 26); however, the concentration of TG2 at the cell periphery is more dramatic in pri-

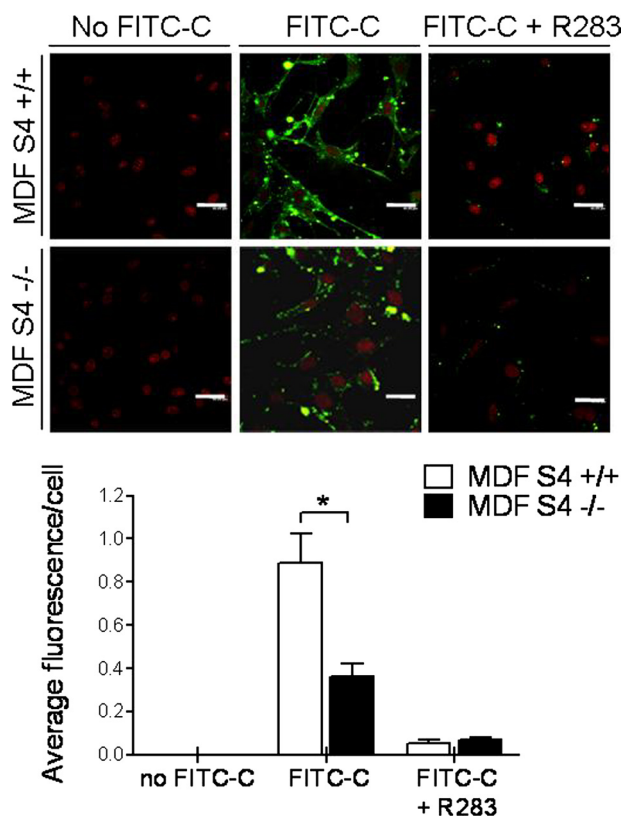


**FIGURE 5. Visualization of *in situ* TG2 activity in wild-type and syndecan-4-null dermal fibroblasts.** *In situ* TG2 activity of S4<sup>+/+</sup> and S4-null MDF was visualized by the incorporation of fluorescein-cadaverine into endogenous substrates. R-283, a site-specific inhibitor of TG activity was used as a control at 200  $\mu$ M. Nuclei were stained with propidium iodide to facilitate cell counting. The average fluorescence produced by fluorescein excitation was quantified by Leica TCSNT image processing in five random fields and expressed as mean fluorescence/cell. \*, significantly different TG2 activity ( $p < 0.05$ ). The bars correspond to 40  $\mu$ m.

mary fibroblasts, as shown here, compared with immortalized fibroblasts where cytosolic TG2 is predominant (7, 8, 26). We next studied whether syndecan-4 co-localized with TG2 in MDF. Double immunolabeling showed that antibodies against TG2 and syndecan-4 co-localized at large cell-matrix adhesion structures (Fig. 7C, arrows). To specifically detect secreted, matrix-bound TG2, cells were incubated with anti-TG2 antibody before cell fixation, as described (7, 9, 26), which revealed a much lower level of extracellular TG2 in syndecan-4-null MDF compared with wild-type MDF (Fig. 7D and supplemental Fig. S8). These findings were consistent with the lower level of cell-surface TG2 activity measured in syndecan-4-null MDF compared with wild-type MDF (Fig. 4A).

Because TG2 was not found on the surface and matrix of syndecan-4-null MDF to the same extent as wild-type MDF, we analyzed whether it was retained intracellularly. Wild-type and syndecan-4-null MDF were detached with non-enzymatic solution, to preserve cell-surface components, solubilized, and fractionated into cytosol and membrane fractions; equal weights of proteins were then fractionated and loaded onto a SDS-polyacrylamide gel in the same amount. We found that the membrane fractions of syndecan-4-null MDF contained a significantly lower amount of TG2 antigen and activity than the membrane fractions of wild-type MDF (Fig. 7, E and F). Conversely, the

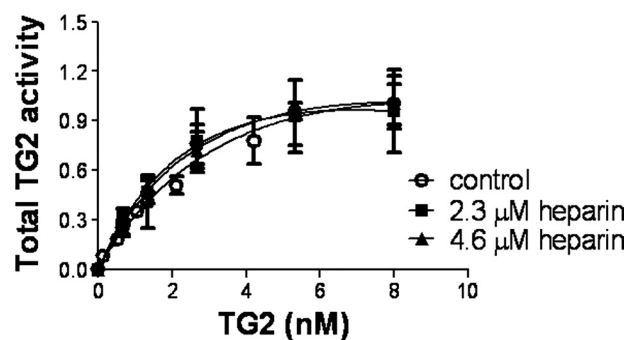


**FIGURE 6. Heparin binding does not affect the cross-linking activity of purified TG2.** The cross-linking activity of purified TG2 was assayed in the absence and presence of heparin as described under "Experimental Procedures." Data are the mean values  $\pm$  S.D. of a representative experiment undertaken in triplicate.  $p > 0.05$ .

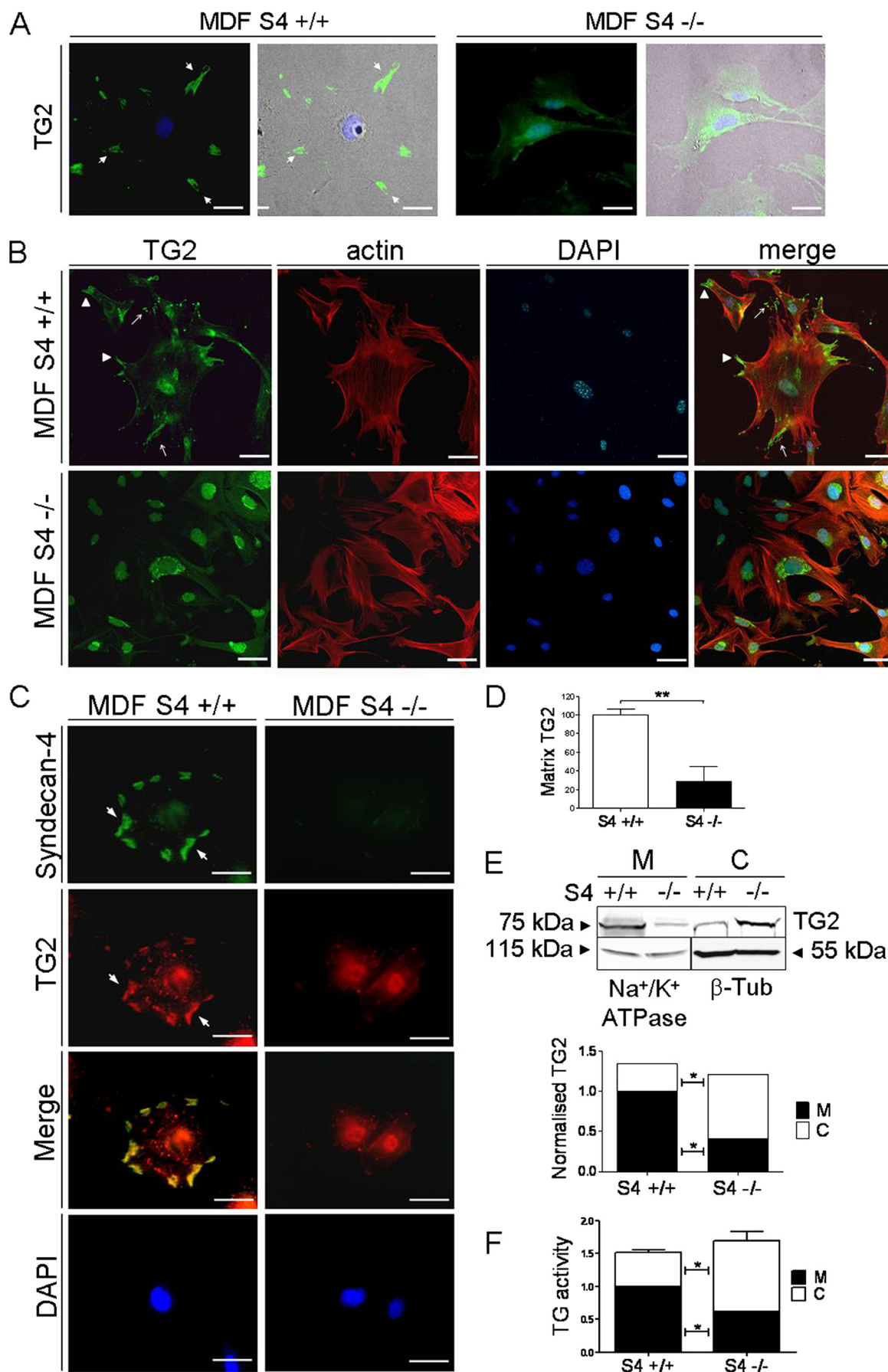
cytosolic fractions of syndecan-4-null MDF had a significantly higher amount of TG2 antigen and activity compared with the cytosolic fractions of wild-type MDF (Fig. 7, E and F). Equal loading was verified by stripping and reprobing the cytosolic fractions with anti-tubulin antibody and the membrane fractions with anti-Na/K ATPase antibody. The combined level of TG2 activity was not significantly different in wild-type and syndecan-4-null MDF (Fig. 7F), in agreement with measurements of TG2 in total cell lysate shown in Fig. 4B. The specificity of the enzyme activity assay for TG2 was confirmed by the absence of cross-linking activity in TG2<sup>-/-</sup> MEFs compared with wild-type MEFs (supplemental Fig. 7B). These data suggest that syndecan-4 contributes to increase the concentration of TG2 in the membrane and at the cell surface.

## DISCUSSION

The data shown in this study assign to HSPG the function of regulating the cell-surface biological activity and trafficking of TG2. Firstly, we have investigated the binding affinity of TG2 for the HS analogue heparin using solid binding assays and surface plasmon resonance. Kinetic studies demonstrated high affinity of TG2 for heparin, giving dissociation constant values in the nanomolar range. These findings were validated using TG2 binding assays to HS, which are more representative of the GAG chains of cell-surface HSPG, showing that the interaction between TG2 and HS or heparin are of similar strength. In our solid binding experiments, the apparent  $K_d$  for the interaction of TG2 for immobilized heparan sulfate was  $\sim 16$  nM. The  $K_d$  for FN, a well established TG2 binding partner (40, 41) was  $\sim 19$  nM, a value that compares well with those calculated in previous solid-phase binding studies ( $\sim 8$ – $10$  nM) (41). Therefore, our data show for the first time that the affinity of TG2 for HS is strong, and it is comparable to that for FN. As a result, these findings suggest the formation of a possible ternary complex of TG2, FN, and HS, where the affinity of TG2 for HS is comparable to the affinity of TG2 for FN.

Secondly, to support the physiological relevance of the high affinity binding of TG2 to HS, we have shown that cell-surface-associated TG2 is crucial for the cell recognition of immobilized heparin and HS. In the same experiments, cell surface-associated TG2 did not similarly affect recognition of FN (judged by measuring cell attachment), although it did influ-

# Heparan Sulfate Binding of Transglutaminase-2



ence cell spreading. This is not surprising, because it has been shown that expression of antisense RNA for TG2 does not affect cell attachment to FN but results in changes in cell spreading (52). However, the contribution of cell-surface TG2 becomes crucial when the main RGD-dependent adhesion pathway is blocked (13). After showing that cell-surface TG2 interacts with immobilized HS, we have also demonstrated that endogenous TG2 physically co-precipitates with syndecan-4 in cell membranes of different cell types, and that this association is significantly reduced by cleavage of cell-surface HS chains. Because obstruction of the FN recognition site within the N-terminal  $\beta$ -sandwich domain of TG2 (40) did not alter TG2-syndecan-4 co-precipitation, this finding suggests that TG2 directly interacts with the HS chains of syndecan-4. The TG2-syndecan-4 association has been verified by TG2 and syndecan-4 labeling showing that TG2 and syndecan-4 are co-localized at large, peripheral cell-matrix adhesions that determine cell shape (46, 53). Thus the presence of syndecan-4 at focal adhesions (46, 47) may facilitate the recruitment of cell-surface TG2.

Thirdly, to test the hypothesis that HSPGs are involved in the biological enzymatic activity of TG2 we have investigated the role of HS binding on the extracellular cross-linking activity of TG2 in live cells in culture, by using a well established assay (7, 9, 39, 44). This assay specifically measures TG2, as the activity is inhibited by preincubation of cells with anti-TG2 antibody (7, 39), and it is completely abolished by deletion of TG2 in TG2-null MEF. In this study, specific interference with the function of cell-surface HS chains was carried out by both enzymatic digestion and antagonism using surfen, a compound that binds low molecular weight heparin and neutralizes HS-associated cellular responses (51). Recently, surfen was shown to block HS-regulated FGF2 binding and signaling in Chinese hamster ovary cells (51). Neutralization of cell-surface HS chains resulted in a dramatic alteration of extracellular TG2 activity in wild-type fibroblasts. We showed that the HS chains of syndecan-4 controlled a significant portion of the extracellular TG2 activity, because extracellular TG2 transamidation was markedly decreased in syndecan-4-null MDF and was rescued by re-expression of syndecan-4, if the functional role of HS chains was not impaired. Visualization of TG2 activity "in situ" in primary fibroblasts, confirmed that absence of syndecan-4 leads to inhibition of TG2 activity, which was predominant at the cell surface of primary dermal fibroblasts. This finding is consistent with evidence of TG2 externalization and tight control of intra-

cellular TG2 activity by tri- and di-phosphate nucleosides and low  $\text{Ca}^{2+}$  (3, 7, 54). Therefore, syndecan-4 binding plays a major contribution in determining extracellular TG2 activity; however, because alteration of HS chains leads to a more radical effect on TG2 activity we speculate that the binding of TG2 is not exclusive to the HS chains of syndecan-4, and the type of HSPG involved may indeed be cell-specific.

Syndecan-4 has been recently implicated in integrin co-signaling induced by adhesion to an experimental matrix of purified exogenous TG2. In this wounding model of matrix fragmentation, purified guinea pig liver TG2 plays a structural, non-catalytic role (14, 31). We have now identified syndecan-4 as an important binding partner for endogenous, cell-secreted TG2 and shown that this binding has a wider physiological significance on the biological activity of TG2. Therefore, syndecan-4 may act as an overall partner of extracellular TG2, being involved in the structural adhesive and, as reported here, the  $\text{Ca}^{2+}$ -dependent cross-linking activity of TG2.

The present data conclusively point to a direct role of the HS portion of HSPG in the extracellular activity of TG2 in primary fibroblasts. We therefore asked whether this function could be due to the direct influence of HSPG binding on TG2 enzymatic activity or on the cell-surface availability of TG2. We showed that the transamidation activity of TG2 was not affected by heparin binding *per se*, while absence of syndecan-4 led to a marked decrease in TG2 at peripheral adhesions and in the pericellular matrix, with proportional TG2 accumulation in the cytosol. Therefore, our data have revealed that heparin binding influences extracellular TG2 transamidation indirectly, by affecting the targeting of TG2 to the cell surface. The possibility that absence of HS may affect the stability of externalized TG2 was ruled out by finding a consistently similar level of total TG2 in wild-type and syndecan-4 null cells. Previous work with a truncated form of TG2 disabled for FN binding and fused to  $\beta$ -galactosidase, showed a lower level of  $\beta$ -galactosidase activity in COS-7 cells transfected with the truncated form, compared with the full-length form of TG2, suggesting that FN binding is also important for the extracellular localization and/or stability of TG2 (26). The limit of that work was in the possible folding alteration of the mutant TG2. For some unconventionally secreted proteins (like FGF-2) translocation must occur in a folded state, and subsequent work has shown the importance of TG2 conformation for secretion (9). In this study, we conducted the opposite experiment to look at whether cells lacking TG2-binding partners had less cell-sur-

**FIGURE 7. Importance of syndecan-4 in cell-surface TG2 location.** A,  $\text{S4}^{+/+}$  and  $\text{S4}$ -null MDF were fixed, permeabilized, and stained with monoclonal anti-TG2 antibody (Cub7402), which was revealed by using a FITC-conjugated secondary antibody. Nuclei were stained with 4',6-diamidino-2-phenylindole. Specimens were imaged using fluorescence or both phase contrast and fluorescence illumination in combination. The arrows indicate TG2 localization at the cell periphery. The bars correspond to 20  $\mu\text{m}$ . B, TG2 staining was performed as described in A; actin stress fibers were stained using TRITC-phalloidin. Arrowheads indicate TG2 localization at cell-matrix adhesions; small arrows indicate TG2 released in the ECM. The bars correspond to 20  $\mu\text{m}$ . C, TG2 and syndecan-4 were co-immunodetected using Cub7402 and anti-polyclonal anti-syndecan-4 antibody, which were revealed by anti-mouse IgG-Rhodamine RedX and anti-rabbit IgG-Alexafluor488, respectively. Nuclei were stained with 4',6-diamidino-2-phenylindole. The arrows point at the cell-matrix adhesion sites where TG2 and syndecan-4 co-localize. The bars indicate 20  $\mu\text{m}$ . D, for detection of matrix-associated TG2,  $\text{S4}^{+/+}$  and  $\text{S4}$ -null MDF were cultured in the presence of Cub7402 before fixation and incubation with FITC-conjugated secondary antibody. Average signal of matrix TG2 per single cell was quantified in three separate fields and is displayed in the graph. Values are normalized considering  $\text{S4}^{+/+}$  signal as 100. \*\* indicates  $p < 0.01$ . E, analysis of the cellular distribution of TG2 in  $\text{S4}^{+/+}$  and  $\text{S4}$ -null MDF. Cells were fractionated into membrane (M) and cytosolic (C) fractions, as described under "Experimental Procedures." The level of TG2 was then assessed by Western blotting using anti-TG2 antibody and equal loading was verified on a parallel blot of membrane and cytosolic fractions, respectively, immunoprobed with anti-Na/KATPase antibody (membrane marker) and anti-tubulin antibody. F,  $\text{S4}^{+/+}$  and  $\text{S4}$ -null MDF were fractionated and the total TG2 activity assayed as described under "Experimental Procedures." The asterisks indicate a significant difference between  $\text{S4}^{+/+}$  and  $\text{S4}$ -null MDF membrane and cytosolic TG2 ( $p < 0.02$ ). There was no significant difference in the total level of TG2 between the two cell types.

## Heparan Sulfate Binding of Transglutaminase-2

face TG2 and demonstrated that in the absence of syndecan-4, TG2 externalization is reduced. The association of TG2 with FN at the cell surface and in the pericellular matrix was previously reported (7, 26). We have now shown that TG2 also co-localizes with syndecan-4, which in turn also co-associates with early assembled FN (55). Therefore, future investigations are warranted to test whether once syndecan-4 recruits TG2 at the cell surface, it contributes to direct the association of TG2 with FN leading to TG2 deposition into the ECM.

Recent evidence have ascribed a role to HSPG in both membrane secretion and endocytosis (56), raising the possibility that HSPG could influence both the secretion and internalization of TG2. This last possibility is intriguing as Zemskov *et al.* (10) have demonstrated that internalization of TG2 requires the endocytic receptor LRP1, and this receptor has been shown to act in concert with HSPG (57). Although we cannot rule out the possibility of a dual function of HSPG in TG2 externalization and internalization, with our syndecan-4 knockout and HS function-blocking cell models we show that lack of syndecan-4/HS leads to a lower level of cell-surface TG2 and a parallel accumulation of cytosolic TG2. Therefore, our findings support a role for HSPG in the trafficking of TG2 to the cell surface. There are several classified unconventional mechanisms of secretion, involving either import into endosomal subcompartments (e.g. IL $\beta$ 1), direct translocation across the plasma membrane (e.g. Leishmania protein HASPB), exosomes/membrane blebbing (e.g. galectins), or direct translocation across the plasma membrane (e.g. FGF1/2) (58). Recently, cell-surface counter receptors have emerged as essential components of non-conventional secretion for galectin1 and FGF-2 (58, 59). In FGF-2 secretion, cell-surface HS function as an extracellular “molecular trap” driving the membrane transport of fully folded FGF-2 by passive diffusion (60, 61).

Given the length and flexibility of the HS chains, our data suggest that HSPGs, like syndecan-4, act as cell-surface receptors to direct the secretion of TG2 from the plasma membrane to the cell surface, where TG2 is catalytically active and leads to matrix stabilization events, which are essential for tissue function and repair.

*Acknowledgments*—We are indebted to M. Griffin for generously providing cell lines and reagents used in this study. We thank G. Melino (Leicester University, UK) for providing the MEF cell lines; V. Sasselli (National Institute for Medical Research, London, UK) for the support with confocal microscopy; A. Gutierrez (Nottingham Trent University) for advice on binding kinetics; and I. Burhan (Nottingham Trent University) for general technical assistance. We are grateful to J. D. Esko (University of California, San Diego) for critically reading our manuscript. Part of this work was presented at the XIX International Symposium on Glycoconjugates (2007), and it is published as an abstract in *Glycoconjugate J.*

## REFERENCES

1. Aeschlimann, D., and Thomazy, V. (2000) *Connect. Tissue Res.* **41**, 1–27
2. Lorand, L., and Graham, R. M. (2003) *Nat. Rev. Mol. Cell Biol.* **4**, 140–156
3. Smethurst, P. A., and Griffin, M. (1996) *Biochem. J.* **313**, 803–808
4. Nakaoka, H., Perez, D. M., Baek, K. J., Das, T., Husain, A., Misono, K., Im, M. J., and Graham, R. M. (1994) *Science* **264**, 1593–1596
5. Liu, S., Cerione, R. A., and Clardy, J. (2002) *Proc. Natl. Acad. Sci. U.S.A.* **99**,

- 2743–2747
6. Feng, J. F., Rhee, S. G., and Im, M. J. (1996) *J. Biol. Chem.* **271**, 16451–16454
7. Verderio, E., Nicholas, B., Gross, S., and Griffin, M. (1998) *Exp. Cell Res.* **239**, 119–138
8. Akimov, S. S., Krylov, D., Fleischman, L. F., and Belkin, A. M. (2000) *J. Cell Biol.* **148**, 825–838
9. Balklava, Z., Verderio, E., Collighan, R., Gross, S., Adams, J., and Griffin, M. (2002) *J. Biol. Chem.* **277**, 16567–16575
10. Zemskov, E. A., Mikhailenko, I., Strickland, D. K., and Belkin, A. M. (2007) *J. Cell Sci.* **120**, 3188–3199
11. Martinez, J., Chalupowicz, D. G., Roush, R. K., Sheth, A., and Barsigian, C. (1994) *Biochemistry* **33**, 2538–2545
12. Chau, D. Y., Collighan, R. J., Verderio, E. A., Addy, V. L., and Griffin, M. (2005) *Biomaterials* **26**, 6518–6529
13. Verderio, E. A., Telci, D., Okoye, A., Melino, G., and Griffin, M. (2003) *J. Biol. Chem.* **278**, 42604–42614
14. Telci, D., Wang, Z., Li, X., Verderio, E. A., Humphries, M. J., Baccarini, M., Basaga, H., and Griffin, M. (2008) *J. Biol. Chem.* **283**, 20937–20947
15. Verderio, E. A., Johnson, T., and Griffin, M. (2004) *Amino. Acids* **26**, 387–404
16. Haroon, Z. A., Hettasch, J. M., Lai, T. S., Dewhirst, M. W., and Greenberg, C. S. (1999) *FASEB J.* **13**, 1787–1795
17. Johnson, T. S., El-Koraie, A. F., Skill, N. J., Baddour, N. M., El Nahas, A. M., Njiloma, M., Adam, A. G., and Griffin, M. (2003) *J. Am. Soc. Nephrol.* **14**, 2052–2062
18. Grenard, P., Bresson-Hadni, S., El Alaoui, S., Chevallier, M., Vuitton, D. A., and Ricard-Blum, S. (2001) *J. Hepatol.* **35**, 367–375
19. Griffin, M., Smith, L. L., and Wynne, J. (1979) *Br. J. Exp. Pathol.* **60**, 653–661
20. Richards, R. J., Masek, L. C., and Brown, R. F. (1991) *Toxicol. Pathol.* **19**, 526–539
21. Thomázy, V., and Fésüs, L. (1989) *Cell Tissue Res.* **255**, 215–224
22. Nicholas, B., Smethurst, P., Verderio, E., Jones, R., and Griffin, M. (2003) *Biochem. J.* **371**, 413–422
23. Skill, N. J., Johnson, T. S., Coutts, I. G., Saint, R. E., Fisher, M., Huang, L., El Nahas, A. M., Collighan, R. J., and Griffin, M. (2004) *J. Biol. Chem.* **279**, 47754–47762
24. Ikura, K., Yokota, H., Sasaki, R., and Chiba, H. (1989) *Biochemistry* **28**, 2344–2348
25. Muesch, A., Hartmann, E., Rohde, K., Rubartelli, A., Sitia, R., and Rapoport, T. A. (1990) *Trends Biochem. Sci.* **15**, 86–88
26. Gaudry, C. A., Verderio, E., Aeschlimann, D., Cox, A., Smith, C., and Griffin, M. (1999) *J. Biol. Chem.* **274**, 30707–30714
27. Signorini, M., Bortolotti, F., Poltronieri, L., and Bergamini, C. M. (1988) *Biol. Chem. Hoppe Seyler* **369**, 275–281
28. Gambetti, S., Dondi, A., Cervellati, C., Squerzanti, M., Pansini, F. S., and Bergamini, C. M. (2005) *Biochimie. (Paris)* **87**, 551–555
29. Bishop, J. R., Schuksz, M., and Esko, J. D. (2007) *Nature* **446**, 1030–1037
30. Morgan, M. R., Humphries, M. J., and Bass, M. D. (2007) *Nat. Rev. Mol. Cell Biol.* **8**, 957–969
31. Verderio, E. A., Scarpellini, A., and Johnson, T. S. (2008) *Amino. Acids* **36**, 671–677
32. Echtermeyer, F., Streit, M., Wilcox-Adelman, S., Saoncella, S., Denhez, F., Detmar, M., and Goetinck, P. (2001) *J. Clin. Invest.* **107**, R9–R14
33. Ishiguro, K., Kadomatsu, K., Kojima, T., Muramatsu, H., Tsuzuki, S., Nakamura, E., Kusugami, K., Saito, H., and Muramatsu, T. (2000) *J. Biol. Chem.* **275**, 5249–5252
34. De Laurenzi, V., and Melino, G. (2001) *Mol. Cell Biol.* **21**, 148–155
35. Scotchford, C. A., Cascone, M. G., Downes, S., and Giusti, P. (1998) *Biomaterials* **19**, 1–11
36. Verderio, E., Coombes, A., Jones, R. A., Li, X., Heath, D., Downes, S., and Griffin, M. (2001) *J. Biomed. Mater. Res.* **54**, 294–304
37. Mahoney, D. J., Whittle, J. D., Milner, C. M., Clark, S. J., Mulloy, B., Buttle, D. J., Jones, G. C., Day, A. J., and Short, R. D. (2004) *Anal. Biochem.* **330**, 123–129
38. Germack, R., and Dickenson, J. M. (2006) *J. Pharmacol. Exp. Ther.* **316**, 392–402

39. Jones, R. A., Nicholas, B., Mian, S., Davies, P. J., and Griffin, M. (1997) *J. Cell Sci.* **110**, 2461–2472
40. Hang, J., Zemskov, E. A., Lorand, L., and Belkin, A. M. (2005) *J. Biol. Chem.* **280**, 23675–23683
41. Radek, J. T., Jeong, J. M., Murthy, S. N., Ingham, K. C., and Lorand, L. (1993) *Proc. Natl. Acad. Sci. U.S.A.* **90**, 3152–3156
42. Rudd, T. R., Guimond, S. E., Skidmore, M. A., Duchesne, L., Guerrini, M., Torri, G., Cosentino, C., Brown, A., Clarke, D. T., Turnbull, J. E., Fernig, D. G., and Yates, E. A. (2007) *Glycobiology* **17**, 983–993
43. Gronthos, S., Stewart, K., Graves, S. E., Hay, S., and Simmons, P. J. (1997) *J. Bone Miner. Res.* **12**, 1189–1197
44. Heath, D. J., Downes, S., Verderio, E., and Griffin, M. (2001) *J. Bone Miner. Res.* **16**, 1477–1485
45. Ott, V. L., and Rapraeger, A. C. (1998) *J. Biol. Chem.* **273**, 35291–35298
46. Longley, R. L., Woods, A., Fleetwood, A., Cowling, G. J., Gallagher, J. T., and Couchman, J. R. (1999) *J. Cell Sci.* **112**, 3421–3431
47. Echtermeyer, F., Baciú, P. C., Saoncella, S., Ge, Y., and Goetinck, P. F. (1999) *J. Cell Sci.* **112**, 3433–3441
48. Greene, D. K., Tumova, S., Couchman, J. R., and Woods, A. (2003) *J. Biol. Chem.* **278**, 7617–7623
49. Johnson, T. S., Skill, N. J., El Nahas, A. M., Oldroyd, S. D., Thomas, G. L., Douthwaite, J. A., Haylor, J. L., and Griffin, M. (1999) *J. Am. Soc. Nephrol.* **10**, 2146–2157
50. Rock, M. J., Cain, S. A., Freeman, L. J., Morgan, A., Mellody, K., Marson, A., Shuttleworth, C. A., Weiss, A. S., and Kielty, C. M. (2004) *J. Biol. Chem.* **279**, 23748–23758
51. Schuksz, M., Fuster, M. M., Brown, J. R., Crawford, B. E., Ditto, D. P., Lawrence, R., Glass, C. A., Wang, L., Tor, Y., and Esko, J. D. (2008) *Proc. Natl. Acad. Sci. U.S.A.* **105**, 13075–13080
52. Stephens, P., Grenard, P., Aeschlimann, P., Langley, M., Blain, E., Errington, R., Kipling, D., Thomas, D., and Aeschlimann, D. (2004) *J. Cell Sci.* **117**, 3389–3403
53. Zamir, E., and Geiger, B. (2001) *J. Cell Sci.* **114**, 3577–3579
54. Begg, G. E., Holman, S. R., Stokes, P. H., Matthews, J. M., Graham, R. M., and Iismaa, S. E. (2006) *J. Biol. Chem.* **281**, 12603–12609
55. Baciú, P. C., and Goetinck, P. F. (1995) *Mol. Biol. Cell* **6**, 1503–1513
56. MacArthur, J. M., Bishop, J. R., Stanford, K. I., Wang, L., Bensadoun, A., Witztum, J. L., and Esko, J. D. (2007) *J. Clin. Invest.* **117**, 153–164
57. Mahley, R. W., and Ji, Z. S. (1999) *J. Lipid Res.* **40**, 1–16
58. Nickel, W. (2007) *J. Cell Sci.* **120**, 2295–2299
59. Seelenmeyer, C., Wegehingel, S., Tews, I., Künzler, M., Aebi, M., and Nickel, W. (2005) *J. Cell Biol.* **171**, 373–381
60. Backhaus, R., Zehe, C., Wegehingel, S., Kehlenbach, A., Schwappach, B., and Nickel, W. (2004) *J. Cell Sci.* **117**, 1727–1736
61. Zehe, C., Engling, A., Wegehingel, S., Schäfer, T., and Nickel, W. (2006) *Proc. Natl. Acad. Sci. U.S.A.* **103**, 15479–15484